

TITANIUM HYDRIDE AND HYDROGEN CONCENTRATION IN ACID ETCHED TITANIUM AND TITANIUM ALLOY IMPLANTS: A COMPARATIVE ANALYSIS OF 5 IMPLANT SYSTEMS.

S. Szmukler-Moncler ^{1,2}, M. Bischof ^{3,4}, R. Nedir ^{3,4}, M. Ermrich ⁵

¹ Dpt of Stomatology & Maxillo-facial Surgery, UFR 068, University of Paris 6, France

² Dpt of Odontology, Section of Implantology and Oral Rehabilitation, Galeazzi Orthopedic Institut, University of Milano, Milano, Italy

³ Swiss Dental Clinics Group, CdR, 3 rue du Collège, CH-1800 Vevey, Switzerland

⁴ Dpt of Stomatology and Oral Surgery, School of Dental Medicine, University of Geneva, Switzerland

⁵ X-Ray Laboratory Dr. Ermrich, Reinheim/Odw, Germany

Correspondence author:

Dr Serge Szmukler-Moncler,
In Intersack 32,
CH- 4103 Ettingen-Basel, Switzerland
Tel + 41 79 504 64 57
E-mail : ssm@bluewin.ch

TITANIUM HYDRIDE AND HYDROGEN CONCENTRATION IN ACID ETCHED TITANIUM AND TITANIUM ALLOY IMPLANTS: A COMPARATIVE ANALYSIS OF 5 IMPLANT SYSTEMS.

Abstract

Background

Acid etching is a popular method to texture the surface of dental implants. During etching, the titanium oxide protective layer is dissolved and native Hydrogen ions are released. These small ions are diffusing into the unprotected implant surface, enrich the implant surface with Hydrogen and form a layer of titanium hydride (TiH) at the implant surface. The aim of this study was to measure the concentration of TiH at the implant surface and the total concentration of Hydrogen for various commercially available implants, made of either cp titanium or titanium alloy.

Material & Methods

3 implants issued from 3 distinct batches were selected from 5 commercially available implant systems with etched surfaces. Implants were made of titanium (Straumann-SLA, Ankylos-Cell Plus, 3i-Osseotite) or titanium alloy (3i-Prevail, MIS-Biocom). X-Ray diffraction was conducted on 2 implants of each implant system to determine the compounds present at the implant surface. Based on a Ti/TiH₂ calibration curve, the concentration of the hydride compound was determined. The concentration of Hydrogen in these implants was also measured.

Results

TiH was present on all cp titanium implants. Concentration varied between 5 to 37 %. No TiH was found on the alloyed implants. H concentration varied between 43 to 108 ppm, no difference was found between the cp titanium and the alloy.

Discussion

The low solubility of H in α -Titanium is responsible for precipitation of H into TiH. The sub-surface is enriched in TiH_{2-x} according to the vigor of the etching conditions. High solubility of H in the β -titanium phase of the $\alpha+\beta$ alloy prevents H precipitation into TiH. All implants, even those lacking TiH on the surface were enriched with H. In all implants, Hydrogen concentration was within the normative limit of 130 ppm.

Conclusion

All implants were enriched in Hydrogen because of the acid etching surface treatment and were within the normative tolerance of 130 ppm. TiH precipitation was recorded on the cp titanium implants but non on the alloyed implants.

Key words : acid etching, Osseotite, sandblasting, SLA, surface treatment, Titanium hydride, titanium alloy, Xray diffraction, H concentration

Introduction

Implant surface modulates bone response¹⁻⁴ and implant anchorage^{5,6}. This brought dental implant manufacturers to implement rough titanium surfaces instead of machined ones. Sandblasting and plasma-spraying have been used for many years^{7,8} to roughen implant surfaces but recently, acid etching gained in popularity among manufacturers^{4, 9-12}.

Acid etching is a subtractive method^{3,12} and surface topography results from a strong corrosion process that creates pits of various dimensions¹²⁻¹⁴. Surface etching takes place when strong acidic conditions with $\text{pH} < 0$ are met, at temperatures varying from room temperature to boiling. Before attacking the metallic titanium, the acids must first dissolve the protective titanium oxide layer. During the course of the corrosion process of titanium, native hydrogen ions (H^+) are released¹⁵. These small ions are diffusing rapidly into the metal because it is left without its dense protective oxide layer; the sub-surface is then enriched with hydrogen^{9,16,17}. When saturation in hydrogen (H) is reached, titanium hydride is formed. Over several microns depth, the composition of the sub-surface is altered¹⁷; it might end up with an up to 40 % titanium hydride layer^{9,13}.

Normative specification bodies like DIN and ASTM regulate the concentration of hydrogen that is tolerated in titanium. The reason is that above a given concentration, hydrogen precipitates into titanium hydride needles¹⁵ and can dramatically affect the fatigue mechanical properties of titanium; the latter is better known as hydrogen embrittlement of titanium¹⁵. In finished products made out of titanium like dental implants, DIN (17850, 17851) and ASTM (F67-89 and F 468) are limiting the concentration of Hydrogen to 130 and 150 ppm, respectively.

A previous paper¹² showed that the surface topography of etched titanium implants varies dramatically because distinct etching conditions are implemented. According to the acid mixture, the etching temperature and time, the surface attack can be mild, moderate or strong¹². Therefore, it was deemed interesting to determine the surface composition of several titanium implant systems displaying distinct surface topographies. It was also aimed to determine if these acid etched implants are complying with the normative content of hydrogen.

The aim of this study was, therefore, to compare 5 implant systems in measuring, 1) the surface composition of the etched implants, i.e. the concentration of titanium hydride at the surface, 2) the concentration of hydrogen in the implants.

Material and methods

Implants

Three commercially implants from 5 implant systems were obtained. Each one had a different lot number and a distinct sterilization expiration date. This was to ensure that the implants were manufactured from 3 distinct batches. Three implant systems were made of cp titanium and 2 were made of titanium grade 5, an alloy with aluminum (6%) and vanadium (4%).

Ankylos Cell Plus implants

These implants (Dentsply-Friatech AG, Mannheim, Germany) are made of cp titanium grade 4. The surface is sandblasted and acid etched; no details of the etching process could be found in the literature or in the manufacturer's advertisement. The implants were 9, 11 and 14 mm long and 7 mm in diameter.

3i Osseotite implants

These implants (3i, Palm Beach Gardens, FL, USA) are made of cp titanium grade 3; the surface is prepared by dual thermo-etching. According to Beatty ¹⁸, the implant surface is successively immersed in a 15 % HF bath to remove the native titanium oxide layer and then etched in a mixture of H₂SO₄/HCl acids (ratio of 6:1), heated at 60-80 °C for 3-10 minutes to create the surface texture. The implants were all 8.5 mm long and 3.3 mm in diameter.

Straumann SLActive implants

These implants (Straumann AG, Basel, Switzerland) are made of cold-worked cp titanium grade 4. According to Steinemann and Simpson ¹⁹, the implant surface is sandblasted with large grit (0.25-0.50 mm) alumina and etched in a boiling mixture of HCl/H₂SO₄. Etching conditions of 125-130°C during 5 minutes have been reported by Wong et al ²². After etching, it is protected from any contact with air to avoid a carbon contamination of the highly reactive surface; it is then packaged and stored in a saline solution ²⁰. The implants were 10, 12 and 14 mm long and 4.8 mm in diameter.

3i Osseotite-Prevail implants

These implants (3i, Palm Beach Gardens, FL, USA) are made of titanium grade 5. According to Tait et al. ²¹, the implant surface is successively immersed in a 7-8 wt % HF bath for about 1 mn to remove the native titanium oxide layer. Then, it is etched in a mixture of HCl/F acids, during 20 mn at room temperature to create the surface texture. The implants were all 13 mm long and 4.1 mm in diameter.

MIS Biocom implants

These implants (MIS, Shlomi, Israel) are made of titanium grade 5. The surface is sandblasted and acid etched, no details of the etching process could be found in the literature or in the manufacturer's advertisement. The implants were all 16 mm long and 3.75 mm in diameter.

Scanning electron microscopy

The implants were observed with a Philips XL 20 scanning electron microscope (FEI, Eindhoven, The Netherlands). The implants were fixed to an aluminum sample holder on a conducting paste with the long axis parallel to the implant holder. Implants were removed from their sterile package and immediately fixed to the implant-holder just before placement in the microscope chamber. Observation was conducted at 20 KeV with a taking-off angle of 30 degrees, magnification varied from x 17 to x 4000.

X-ray Diffraction

Samples were analyzed with a Θ/Θ - diffractometer (STOE & Cie, Darmstadt, Germany) using Cu- K α radiation ($\lambda = 1,5418\text{\AA}$, U = 40kV, I = 40mA) and a secondary beam monochromator (plane Graphite (002)) in front of the scintillation counter. The diffraction patterns were obtained over a 2Θ angle of 30-80° with steps of 0.04° and 8 seconds per step. The investigated implant surface was set perpendicular to the radiation beam, 2 implants per system were analyzed.

Implants were then heat-treated at 250°C for 3 hours and again analyzed. The aim of the heat treatment was to decompose the titanium hydride layer when present and to get back the original titanium surface before etching ¹³.

To perform the quantitative phase analysis, a calibration curve was set up with mixtures of Ti hydride and Ti powder (DOT, Rostock, Germany). The Ti powder was obtained by heating the hydride powder in vacuum at 300°C for 10 hours, complete decomposition of the hydride phase was verified. The 2 powders were then mixed at concentrations varying from 0 to 50 % [m/m], the incremental step was 10 % [m/m]. Then, the ratios of the sums of the integral intensities of the reflections of each phase were calculated. To minimize the influence of preferred orientation, no overlapping reflection was used. The ratios were calculated with Ti (002), (101), (102), (110), (112), (201) and TiH (200), (220). With this method, the results could be independent of primary beam intensity, slits, measuring time parameters and the radiated area on the sample. The calibration curve was based on the average of 2 measurements performed for each concentration of the TiH/Ti mixture.

Concentration of Hydrogen

The concentration of Hydrogen in the implants was measured according to ASTM E1147-05 by the inert gas fusion thermal conductivity/infrared detection method; a RH 404 Leco (Leco Corp, St Joseph, MI, USA) was used. Two implants of each implant system served to assess the concentration in each implant group.

Results

Scanning electron microscopy

Figures taken at the 5 implant systems are shown in **Fig 1a-e**. Remains of the sandblasting material were found on all sandblasted surfaces. For the Cell-Plus (**Fig 1a**) and SLActive (**Fig 1b**) implants, sandblasting and strong etching led to formation of a combination of a macro- and micro-topography. The latter was similar to the classical SLA surface ¹². The micro-topography of the Osseotite implants is the result of moderate etching (**Fig 1c**). Etching was moderate as well for the Prevail Osseotite implants made of titanium alloy, but the surface aspect was different than the Osseotite implant made of cp titanium (**Fig 1c**). The micro-topography consisted in rounded cavities and protruding white spots (**Fig 1d**); the latter correspond to the β -phase that is more resistant to etching than the α -phase. Etching conditions of the BioCom implants (**Fig 1e**) were stronger; the β -phase was completely dissolved, in contrast to the previous implant. The micro-topography obtained by strong etching was superimposed on the macro-topography obtained by

sandblasting.

X-ray Diffraction

The XRD patterns of the 3 implants made of cp titanium matched the peaks of PDF 44-1294 corresponding to hexagonal α -titanium. Additional peaks that did not belong to titanium were also found. Taking into account an overlapping peak with (100) Ti, they matched the peaks of PDF 78-2216 corresponding to cubic TiH_{1.5} (**Fig 2a-c**). A heat treatment of 250°C for 3 hours made the peaks belonging to TiH disappear (**Fig 2a-c**), leaving only the pristine titanium peaks. This allowed also determining the relative intensity ratios of the grown TiH. On the SLActive implants, additional peaks of Halide (NaCl) belonging to the saline storing liquid were found (**Fig 2b**).

The XRD patterns of the 2 implants made of TAV matched the peak of titanium; the main peak of the β -phase is overlapping with (002) Ti of the α -phase and could not be discriminated. In contrast to cp Ti implants however, no additional peak was found on the TAV implants (**Fig 2d,e**).

The TiH calibration curve was plotted with the integral intensity ratio of the non overlapping TiH and Ti peaks (**fig 3**). The ratio corresponding to each implant system was then matched on the calibration curve. Minor and major variations were found between samples belonging to the same implant system (**Table 1**). The hydride concentration varied from 5 to 8 % for the Osseotite implants; it was 37 and 19 % for the SLActive implants and 34 and 30 % for the Cell-Plus implants.

H concentration

Table 1 shows the H concentration measured for each implant and the mean calculated for each implant type. The lowest concentration of Hydrogen was 43 ppm, it was measured for a Straumann SLActive implant; highest concentration was 106 ppm, measured for a MIS BioCom implant. No implant reached the critical concentration of 130 ppm of hydrogen.

Discussion

The absorption of H of surface etched dental implants made out of titanium must be carefully monitored since H in excess might lead to precipitation of TiH and further too possible hydrogen embrittlement¹⁵. To our knowledge, this is the first paper to address the concentration of TiH in dental implants as a finished product. Previous papers have showed the existence of an enriched amount of H in SLA treated titanium samples^{16, 17} and documented the presence of a TiH layer in the sub-surface of these samples^{9, 13, 17}. However, no comparison has been undertaken so far to compare the surface composition and hydrogen uptake of various implant systems.

The protocol of the present study paid attention to compare implants made of cp Ti and TAV with strong and moderate etching conditions. These conditions were assessed by analyzing the surface topography by SEM and comparing the data available on the etching conditions. Moderate etching conditions were attributed to the cp and alloyed titanium Osseotite implants because of the low temperatures of the etching baths^{18,21} and the

observed topography. Strong etching conditions were attributed to the cp titanium SLA implants¹² because of the boiling temperature of the acids²² and the surface aspect¹². Although the etching conditions of the Cell Plus implants are not available, comparison with the SLA surface indicates comparable strong etching conditions. These are necessary to remove most of the sandblasting material and carve the titanium surface with deep pores. Similarly, strong etching conditions could also be attributed to the BioCom implants since the β -phase, that was visible on the milder etched Osseotite alloyed implants, was completely removed while carving the surface with pores.

XRD diffraction revealed that all cp Ti implants had various amounts of TiH. Strong etching conditions led to the presence of 19-37 % of TiH, while moderate etching decreased the hydride content down to 5 %. Conversely, no TiH was found on the alloyed implants whatever the etching conditions were, moderate for the Prevail or strong for the Biocom implants. Hydrogen solubility is limited in the hexagonal close packed (HCP) structure of α -Ti. At low concentration, H is accommodated at the octahedral interstitial sites and the balance is accommodated in the tetrahedral sites²³. Above 20 ppm however, hydrogen precipitates into TiH²⁴ and the α phase coexists with a non stoichiometric deficient dihydride, the δ -TiH_{2-x} phase²⁵.

On the other hand, H solubility in β -Ti is much higher because the body centered cubic (BCC) structure is able to accommodate more interstitial elements than the HCP. It has been reported that concentration as high as 50 at % do not lead to formation of precipitated TiH²⁶. In the alloyed grade 5 titanium, vanadium is a β -stabilizer element; it leads to formation of biphasic (α + β) titanium, in which the β -phase can amount up to 10 %, depending on the heat treatment history^{27,28}. The β -phase is distributed along the grain boundaries and offers a more open path for H diffusion²⁸. In the TAV alloy, below 650 ppm, H is primarily concentrated in the β -phase and very little goes into the α -phase²⁷. This explains why no precipitated TiH structure was detected on the alloyed implants since the highest H concentration was 108 ppm.

By nuclear reaction analysis, Aronsson et al.¹⁷ measured the Ti/H ratio of the titanium hydride TiH_{2-x} grown on SLA treated surfaces. The structure was found non-stoichiometric and the Ti/H ratio varied from 1.2 to 0.3; it was decreasing from the sub-surface below the oxide layer to 1.25 μ m in depth. In the present study, the TiH on all 3 implant systems made out of cp Ti could be decomposed at 250°C instead of the 400°C required to decompose the stoichiometric TiH₂ hydride²⁹. This confirms the lack of stoichiometry of the hydride grown on the implant surfaces. Noteworthy, the issue of TiH biocompatibility does not need to be addressed since the etched surfaces are separated from the biological environment by a dense stoichiometric titanium oxide layer that prevents any effusion and interaction^{16,17}.

Within the same cp Ti implant system, higher TiH concentration could be related with higher H uptake (**Table 1**). However, stronger etching conditions did not lead necessary to a larger H uptake. Only in the TAV group, stronger etching conditions were found to lead to a larger H uptake. According to the literature, several parameters can influence H absorption²⁴, they are: 1) the grain size (fine absorbs more H than coarse), 2) the form of grain (elongated absorbs more H than equiaxed), 3) the dislocation density (high dislocation density allows higher H absorption), 4) the surface state (sandblasted absorbs more H than pricked), 5) presence of O (rich in O absorbs less H than poor in O), 6) presence of Fe (rich in Fe absorb less H than poor). Therefore, it is difficult to predict which etching

treatment would lead to a larger or a lower H uptake.

Finally, the most important finding of this survey was that all implants, whatever the etching conditions and the material met the 130-150 ppm of H tolerated by DIN and ASTM. Therefore, hydrogen embrittlement because of the etching process should not be expected, especially in the alloyed implants where the normative tolerance may be even higher than 130-150 ppm. Nevertheless, this issue should be addressed by metallographic sections showing the distribution pattern of the TiH needles that cannot be avoided ²⁴.

Conclusion

Whatever etching is strong or moderate, acid etched implants made of cp Ti are covered by a non-stoichiometric layer of TiH. For the alloyed TAV implants, H is absorbed in the β -phase and does not precipitate as titanium hydride. Acid etching to texture implant surface, either moderate or strong, leads to H enrichment, whatever they are made of cp Ti or TAV alloy. For cp Ti, the absorbed H could not be related to the strength of the etching bath.

References

1. Buser D, Schenk RK, Steinemann SG, Fiorellini JP, Fox CH, Stich H. Influence of surface characteristics on bone integration of titanium implants: A histomorphometric study in miniature pigs. *J Biomed Mater Res* 1991;25:889-902.
2. Szmukler-Moncler S, Reingewirtz Y, Weber HP. Bone response to early loading: The effect of surface state. In: Davidovitch Z, Norton LA, editors. *Biological mechanisms of tooth movement & craniofacial adaptation*. Boston: Harvard Society for the Advancement of Orthodontics; 1996. p 611–616.
3. Cochran DL, Schenk RK, Lussi A, Higginbottom FL, Buser D. Bone response to unloaded and loaded titanium implants with a sandblasted and acid-etched surface: A histometric study in the canine mandible. *J Biomed Mater Res A* 1998;40:1-11.
4. Lazzara RJ, Testori T, Trisi P, Porter SS, Weinstein RL. A human histologic analysis of Osseotite and machined surfaces using implants with 2 opposing surfaces. *Int J Periodont Rest Dent* 1999;19:3-16.
5. Klokkevold PR, Johnson P, Dadgostari S, Caputo A, Davies JE, Nishimura RD. Early endosseous integration enhanced by dual acid etching of titanium: A removal torque study in the rabbit. *Clin Oral Implant Res* 2001;12:350-357.
6. Bernard JP, Szmukler-Moncler S, Pessotto S, Vazquez L, Belser UC. The anchorage of Brånemark and ITI implants of various lengths. I. An experimental study in the canine mandible. *Clin Oral Implant Res* 2003;14:593-600.
7. Kirsch A, Ackermann KL. The IMZ osteointegrated implant system. *Dent Clin North Am* 1989;33:733-791.
8. Makkonen T, Holmberg S, Niemi L, Olsson C, Tammissalo T, Peltola J. A 5-Year Prospective Clinical Study of Astra Tech Dental Implants Supporting Fixed Bridges or Overdentures in the Edentulous Mandible. *Clin Oral Impl Res* 1997;8:469-475.
9. Szmukler-Moncler S, Simpson JP. Physicochemical characterization of a titanium textured surface prepared by sandblasting and acid etching. *Transactions 5th World Biomaterials Congress, 1996, May 29-June 2*, 837
10. Lazzara RJ, Testori T, Trisi P, Porter SS, Weinstein RL. A human histologic analysis of Osseotite and machined surfaces using implants with 2 opposing surfaces. *Int J Periodont Rest Dent* 1999;19:3-16.
11. Rocuzzo M, Bunino M, Prioglio F, Bianchi SD. Early loading of sandblasted and acid-etched (SLA) implants: a prospective split-mouth comparative study. *Clin Oral Implants Res* 2001;12:572-578.
12. Szmukler-Moncler S, Testori T, Bernard JP. Etched implants: a comparative surface analysis of four implant systems. *J Biomed Mater Res B* 2004;15:69:46-57.
13. Perrin D, Szmukler-Moncler S, Echikou C, Pointaire P, Bernard JP. Bone response to alteration of surface topography and surface composition of sandblasted and acid etched (SLA) implants. *Clin Oral Implants Res* 2002;13:465-469.
14. Szmukler-Moncler S, Perrin D, Ahossi V, Magnin G, Bernard JP. Biological properties of acid etched titanium implants: effect of sandblasting on bone anchorage. *J Biomed Mater Res B* 2004;15:68:149-59.
15. Donachie MJ Jr. *Titanium: A Technical Guide*. 2nd edition, ASM International, Materials Park, Ohio, 2000.
16. Taborelli M, Jobin M, François P, Vaudaux P, Tonetti M, Szmukler-Moncler S, Simpson JP, Descouts P. Influence of surface treatments developed for oral implants on the physical and biological properties of titanium. (I) Surface characterization. *Clin Oral Implants Res* 1997;8:208-216.

17. Aronsson BO, Hjørvarsson B, Frauchiger L, Taborelli M, Vallotton PH, Descouts P. Hydrogen desorption from sandblasted and acid-etched titanium surfaces after glow-discharge treatment. *J Biomed Mater Res A* 2001;54:20-29.
18. Beaty KD. US patent 5,876,453. Implant surface preparation. March 2, 1999
19. Steinemann SG, Claes L. US patent 5,456,723. Metallic implant anchorable to bone tissue for replacing a broken or diseased bone. October 10, 1995
20. Steinemann SG, Simpson JPS. Preparation of osteophilic surfaces for metallic prosthetic devices anchorable to bone. European Patent 1 023 910 A1, 2000
21. Tait RT, Berckmans BN, Ross TW, Mayfield RL. Surface treatment process for implants made of titanium alloy. United States Patent 20040265780
22. Wong M, Eulenberger J, Schenk R, Hunziker E. Effect of surface topology on the osseointegration of implant materials in trabecular bone. *J Biomed Mat Res* 1995;29:1567-1575.
23. San Martin A, Manchester FD. The H-Ti (Hydrogen-Titanium) system. *J Physic Equilibria* 1987;8:30-42.
24. Livanov VA, Bukhanova AA, Kolachev BA. Hydrogen in Titanium Israel Program for scientific translation LTD, n°2163, D Davey & Co., Israel 1965
25. Dantzer P. High temperature thermodynamics of H₂ and D₂ in titanium, and in dilute titanium oxygen solid solutions. *J Phys Chem Solids* 1983;44:913-923.
26. Shih DS, Birnbaum HK. Evidence of FCC titanium hydride formation in β titanium alloy: An X-ray diffraction study. *Scripta Metallurgica* 1986;20:1261-1264.
27. Pittinato GF, Hanna WD. Hydrogen in β transformed Ti-6Al-4V. *Metallurgical and Materials Transactions B* 1972;3:2905-2909
28. Wu TI, Wu JK. Effects of electrolytic hydrogenating parameters on structure and composition of surface hydrides of cp-Ti and Ti-6Al-4V alloy. *Materials Chemistry and Physics* 2002;74:5-12.
29. Lide D. Handbook of Chemistry and Physics, CRC Press LLC, Boca Raton, FL. USA, 85th edition, 2005.

Captions

Fig 1

SEM micrographs of the implant surfaces.

- a. Ankylos Cell-Plus implant (x 2000).
Strong etching conditions have carved the Ti surface with pores.
- b. Straumann SLActive implant (x 2000).
Sandblasting and etching with boiling acids created this complex topography.
- c. 3i Osseotite cp Ti implant (x 2000)
Moderate etching conditions led to pores of limited dimensions.
- d. 3i Osseotite Prevail TAV implant (x 2000).
Round pores have been created. The white spots belong to the unetched β -phase.
- e. MIS Biocom implant (x 2000)
A strong etching got rid of the β -phase and carved pores in the alloyed material. At this magnification, the effect of sandblasting is not evidenced on this picture.

Fig 2

XRD patterns of the implant surfaces before and after heat treatment.

- a. Ankylos Cell-Plus implant.
TiH peaks are detected before the heat treatment, they have disappeared afterwards.
- b. Straumann SLActive implant.
TiH peaks are present before the heat treatment only. Peaks belonging to NaCl (H = Halide) have been detected after the heat treatment because of the storing liquid in the sterile ampoule.
- c. 3i Osseotite cp Ti implant.
The TiH peaks before the heat treatment are of lower intensity when compared to the 2 previous implants.
- d. 3i Osseotite Prevail TAV implant.
Note the absence of any TiH peak in the alloyed implant.
- e. MIS Biocom implants.
Note the absence of any TiH peak in the alloyed implant.

Fig 3

TiH/Ti calibration curve.

The TiH/Ti ratio increased with the increase of the TiH concentration. Two measurements have been performed for each concentration.

Table 1

Titanium hydride concentration on the implant surface of each implant system and Hydrogen up-take in these implants.

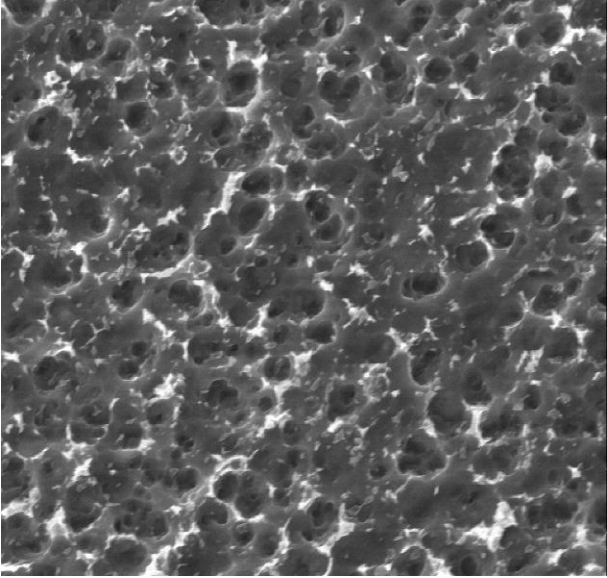


Fig 1 A

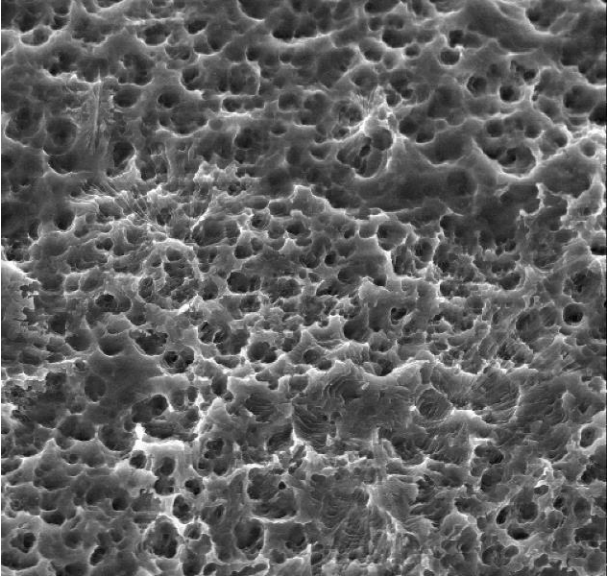


Fig 1 B

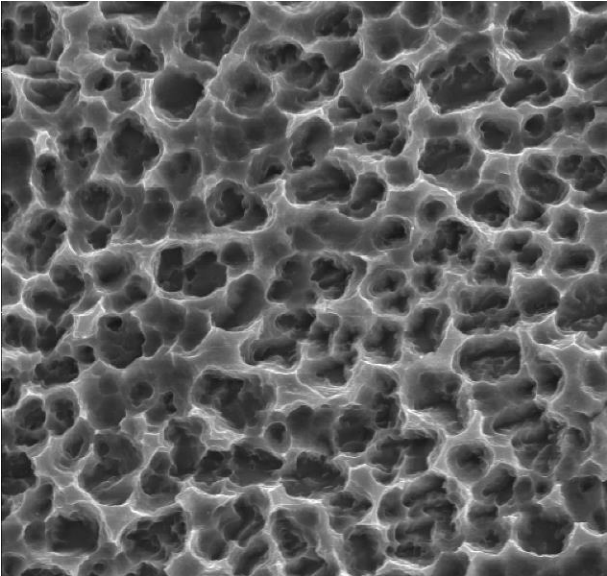


Fig 1 C

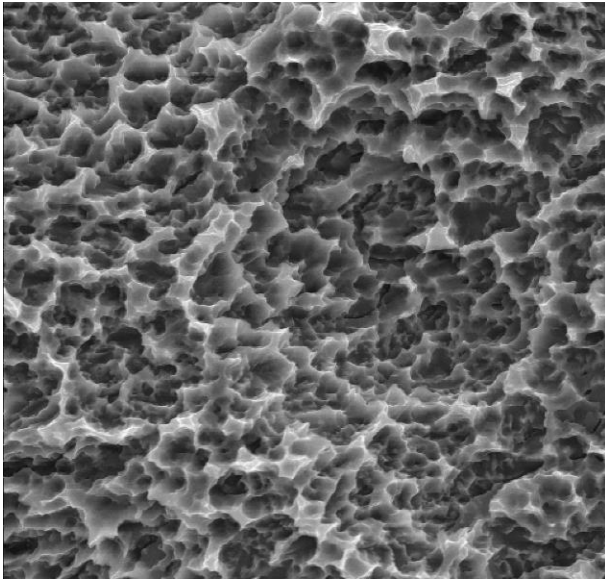


Fig 1D

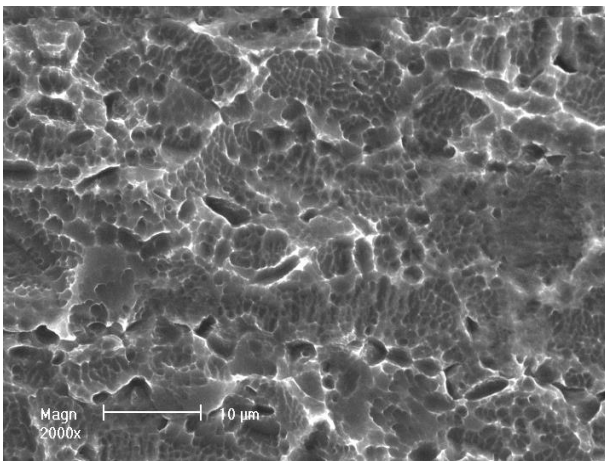


Fig 1E

Fig 1

SEM micrographs of the implant surfaces.

- a. Ankylos Cell-Plus implant (x 2000).
Strong etching conditions have carved the Ti surface with pores.
- b. Straumann SLActive implant (x 2000).
Sandblasting and etching with boiling acids created this complex topography.
- c. 3i Osseotite cp Ti implant (x 2000)
Moderate etching conditions led to pores of limited dimensions.
- d. 3i Osseotite Prevail TAV implant (x 2000).
Round pores have been created. The white spots belong to the unetched β -phase.
- e. MIS Biocom implant (x 2000)
A strong etching got rid of the β -phase and carved pores in the alloyed material. At this magnification, the effect of sandblasting is not evidenced on this picture.

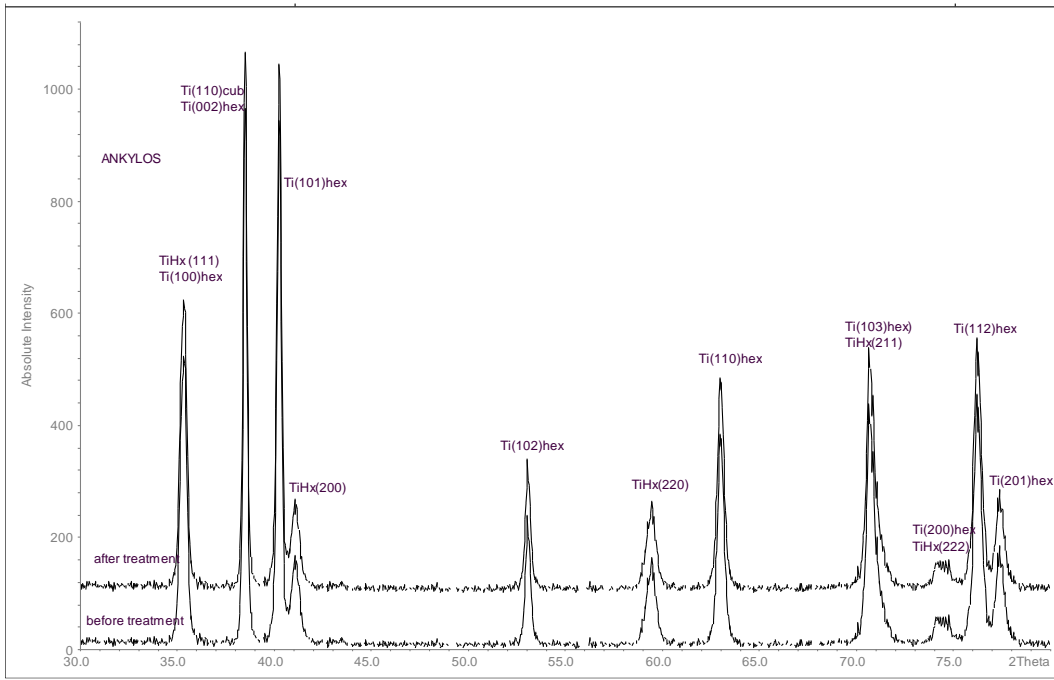


Fig 2A

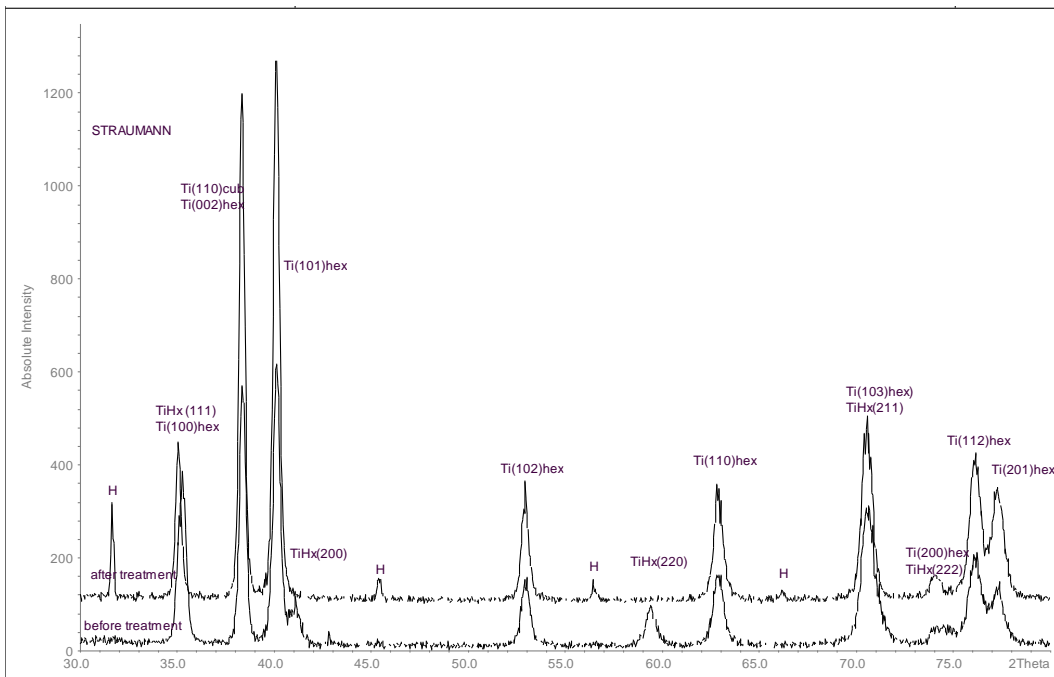


Fig 2B

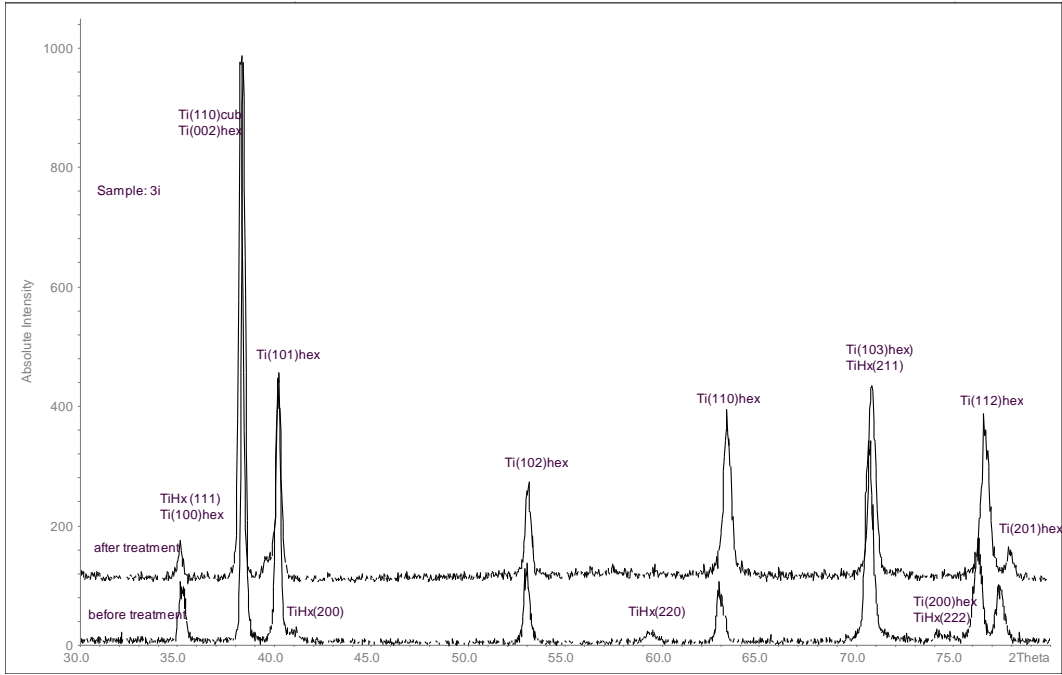


Fig2C

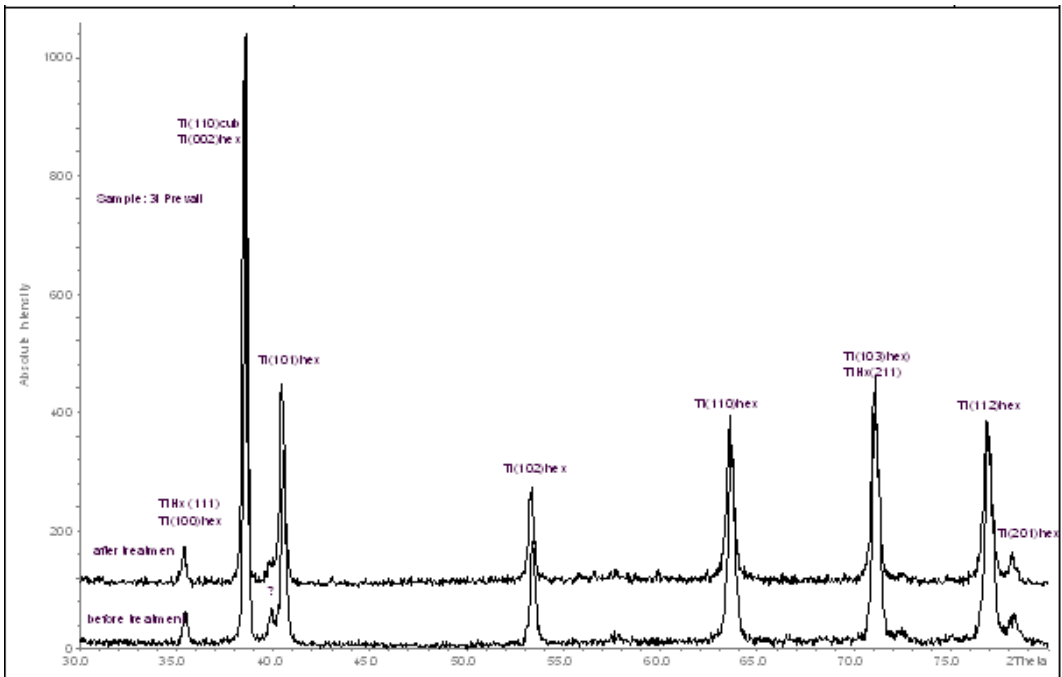


Fig 2D

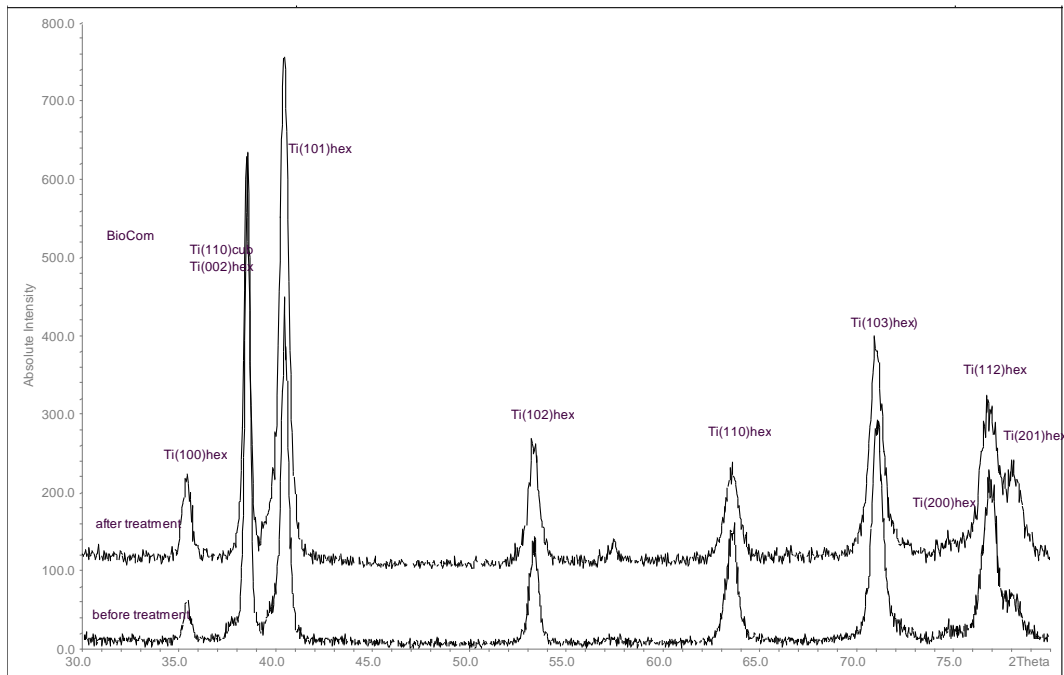


Fig 2E

Fig 2

XRD patterns of the implant surfaces before and after heat treatment.

a. Ankylos Cell-Plus implant.

TiH peaks are detected before the heat treatment, they have disappeared afterwards.

b. Straumann SLActive implant.

TiH peaks are present before the heat treatment only. Peaks belonging to NaCl (H = Halide) have been detected after the heat treatment because of the storing liquid in the sterile ampoule.

c. 3i Osseotite cp Ti implant.

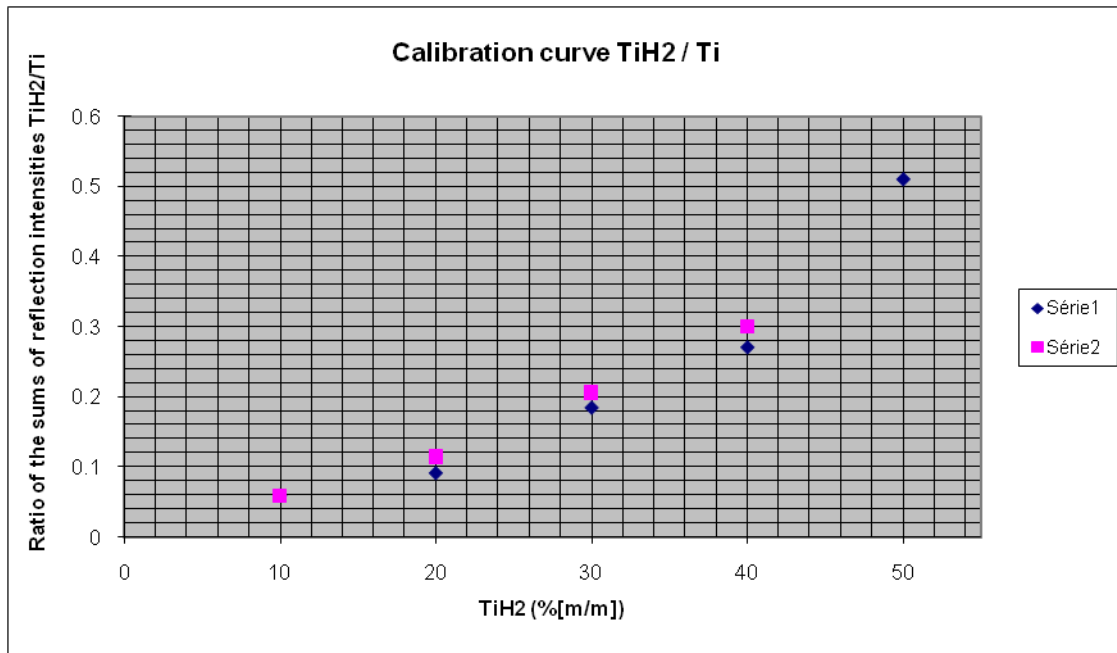
The TiH peaks before the heat treatment are of lower intensity when compared to the 2 previous implants.

d. 3i Osseotite Prevail TAV implant.

Note the absence of any TiH peak in the alloyed implant.

e. MIS Biocom implants.

Note the absence of any TiH peak in the alloyed implant.

**Fig 3**

TiH/Ti calibration curve.

The TiH/Ti ratio increased with the increase of the TiH concentration. Two measurements have been performed for each concentration.

Implants		XRD measurements			Hydrogen concentration (ppm)	
		Concentration of Ti Hydride (%)	Concentration of titanium (%)	Average concentration of Hydride (%)	Concentration of hydrogen	Average concentration of Hydrogen
Straumann	4.8 x 10	37	63	28%	69	56
Straumann	4.8 x 12	19	81			
Osseotite cp	3.3 x 8.5	5	95	6.5%	81	78
Osseotite cp	3.3 x 8.5	8	92			
Ankylos	7.0 x 9.5	34	66	32%	81	69
Ankylos	7.0 x 14	30	70			
Osseotite TAV	4/5/4 X 13	-	100	0%	54	55
Osseotite TAV	4/5/4 X 13	-	100			
Osseotite TAV	4/5/4 X 13	-	100			
BioCom	3.75 x 16	-	100	0%	103	106
BioCom	3.75 x 16	-	100			
BioCom	3.75 x 16	-	100			

Table 1

Titanium hydride concentration on the implant surface of each implant system and Hydrogen up-take in these implants.